2Pb2-6

Three-dimensional numerical analysis of ultrasonic propagation behavior in a powder layer between metals

Daichi Tsunaki[‡], Naoki Mori, and Takahiro Hayashi (Grad. School Eng., Osaka Univ.)

1. Introduction

Selective laser melting (SLM) has been attracting attention as a metal additive manufacturing technology in recent years, but defects inside the manufactured body often become an issue in the new technology. For example, insufficient laser power during the process can lead to metal powder remaining in pores[1]. Laser ultrasonics is one of the defect inspection techniques for quality assurance of the SLM. In the previous study, an imaging method was proposed for voids near surfaces based on local defect resonance occurring when exciting elastic waves[2]. However, the effect of metal powder left inside the defect on the elastic waves has not been fully revealed. In this study, to obtain fundamental knowledge, ultrasonic wave propagation behavior in spherical granular bodies sandwiched between solid blocks is clarified by three-dimensional finite element analysis in the frequency domain.

2. Numerical Models and Methods

As shown in **Fig. 1**, elastic wave propagation was numerically analyzed in the model of a spherical powder layer sandwiched between semi-infinite solid blocks. A unit structure shown in **Fig. 2** was extracted from the entire body to simplify the model, and the side surfaces were set as periodic boundaries. To suppress the effect of reflected waves, absorbing regions were placed outside the solid blocks. The material properties of stainless steel (longitudinal wave velocity 5.66 km/s, transverse wave velocity 3.12 km/s and mass density 7.9 g/cm^3) were used to model the powder and blocks. The diameter of the powder was set as 1 mm, and the sphere and the blocks were assumed to be completely connected. A commercial finite element analysis software COMSOL Multiphysics® was used to perform the numerical simulation. In the frequency domain, a longitudinal wave of a single frequency was emitted from the top surface of the upper block, and the vertical (z direction) displacement amplitude of the transmitted wave across the sphere layer was calculated at point A, which is 1 mm below the top surface of the lower block.

3. Numerical results for a single sphere layer

Fig. 3 shows the numerical results of the z direction displacement amplitude of the transmitted wave obtained in 1 kHz increments from 2.65 MHz to 2.68 MHz. A sharp peak is observed at 2.659 MHz. The distribution of the displacement amplitude near the sphere layer at the peak frequency of 2.659 MHz is shown in **Fig. 4**. The displacement amplitude of the sphere is significantly larger than the displacement amplitude of the incident wave. The sphere appears to show an extensional vibration in the z direction.

Modal analysis for a single sphere was performed to examine the above feature. **Fig. 5** shows a natural vibration mode profile at 2.626 MHz, which indicates an extensional vibration in the z direction. This mode corresponds to a spheroidal mode of an elastic sphere[3]. The transmitted wave across the sphere layer is amplified at 2.659 MHz in Fig. 3 because the spheroidal mode is induced. It is noted that the peak frequency of the transmitted amplitude slightly deviates from the natural vibration frequency probably because the boundary conditions for the sphere in the model analysis and the wave propagation analysis are different.

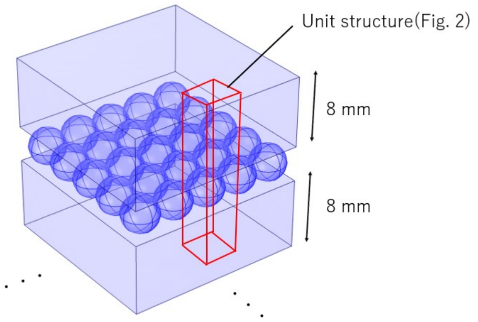

Fig. 1 Schematic of a single sphere layer sandwiched by semi-infinite solid bodies.

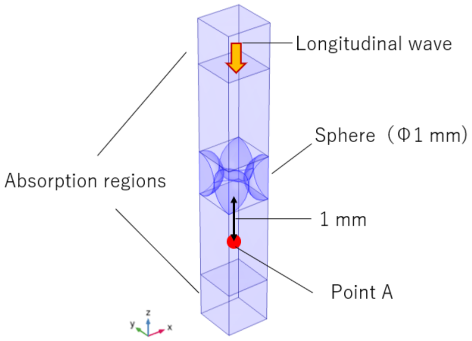

Fig. 2 Unit structure extracted from Fig. 1.

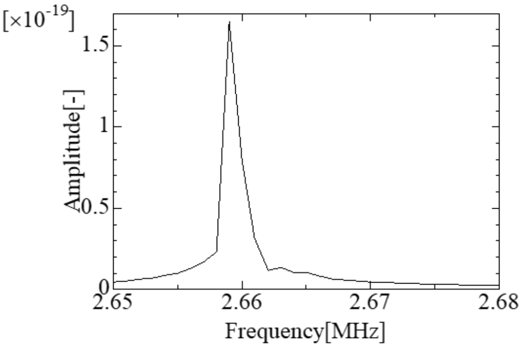

Fig. 3 Amplitude of the *z* direction displacement of the transmitted wave across the single sphere layer.

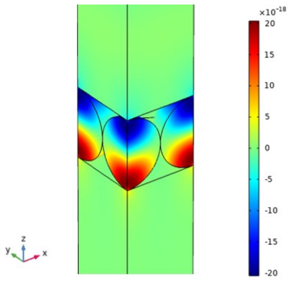

Fig. 4 Distribution of the displacement in the *z* direction at the peak frequency 2.659 MHz.

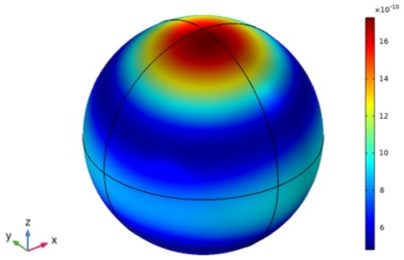

Fig. 5 Displacement distribution at 2.626 MHz obtained by modal analysis for a sphere.

4. Numerical results for a double sphere layer

The numerical analysis was performed for the case of two spheres stacked with the line between the centers of the two spheres parallel to the *z* axis. The *z* direction displacement amplitude of the transmitted wave at point A was analyzed in 1 kHz increments from 2.64 MHz to 2.68 MHz. The obtained results are shown in **Fig. 6**. In the case of the single sphere layer, as shown in Fig. 3, a single peak appears at 2.659 MHz. However, for the double sphere layer, two peaks are observed at 2.649 MHz and 2.663 MHz. The distributions of the *z* direction displacement amplitudes at the two peak frequencies are shown in **Fig. 7**, respectively. The displacement amplitude near the sphere layer locally increases at both peak frequencies. However, the displacement distribution differs depending on the peak frequency. At the peak frequency of 2.649 MHz, the contact points of the two spheres vibrate in the same phase, while at 2.663 MHz, the motions are in the opposite phase.

To further examine this phenomenon, consider the spring-mass system shown in Fig. 7. The spheres and the blocks are modeled by point masses m and fixed rigid walls, respectively. The contact points between the block and the sphere are modeled by springs with spring constant k_1, and that between the two spheres are modeled by a spring with spring constant k_2. This system has two natural angular frequencies

$$\omega_{1,2}=\sqrt{\frac{k_1}{m}},\sqrt{\frac{k_1+2k_2}{m}}. \qquad (1)$$

In the first natural vibration mode, the relative displacement of the point masses is zero, while in the second natural vibration mode, the masses vibrate in the opposite phase. Namely, the natural vibration of this system agrees qualitatively with that of the sphere sandwiched by the blocks shown in Fig. 7. Note that the first mode with angular frequency ω_1 corresponds to the natural vibration of a single point mass, but the displacement amplitude in Fig. 6 does not increase at the peak frequency in Fig. 3. This deviation would be attributed to the modeling of solid blocks as fixed rigid walls.

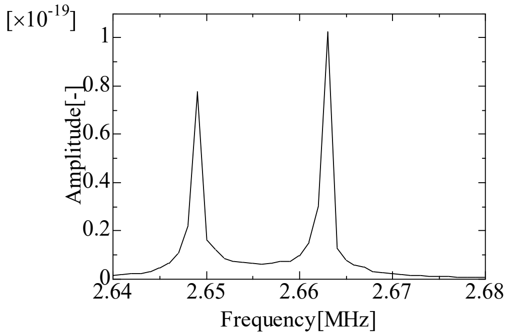

Fig. 6 Amplitude of the *z* direction displacement of the transmitted wave across the double sphere layer.

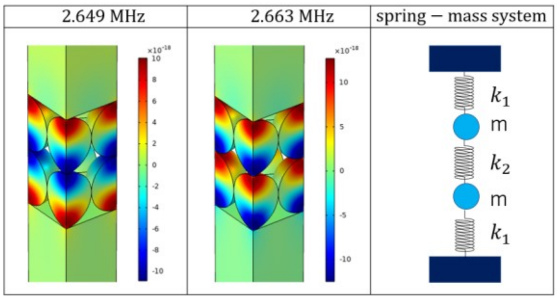

Fig. 7 Displacement distributions in the *z* direction at the two peak frequencies, and schematic of spring-mass system.

References

1. Z. Pitrmuc et al: Materials **15** (2022) 551.
2. T. Hayashi, N. Mori and T. Ueno: Ultrasonics **119** (2022) 106560.
3. L. Saviot and D. B. Murray: Phys. Rev. B **72** (2005) 205433.